Nucleon Transfer with Oxygen Ions Below and Near the Coulomb Barrier*

K. G. Nair, J. S. Blair, W. Reisdorf,† W. R. Wharton,‡ W. J. Braithwaite,§ and M. K. Mehta¶
Department of Physics, University of Washington, Seattle, Washington 98195
(Received 10 May 1973)

Excitation functions have been measured at $\theta_{lab} = 170°$ for the reactions $^{140}Ce(^{16}O, ^{15}N)^{141}Pr$ ($E_{lab} = 56.0$ to 63.0 MeV), $^{88}Sr(^{16}O, ^{15}N)^{89}Y$ (42.5 to 50.0 MeV), and $^{140}Ce(^{18}O, ^{17}O)^{141}Ce$ (56.0 to 61.0 MeV) proceeding to low excited states. Analysis has been made using the sub-Coulomb distorted-wave Born-approximation theory of Buttle and Goldfarb with inclusion of Coulomb correction terms in the form factor and the Buttle-Goldfarb approximation for recoil corrections. Good fits are obtained to the excitation functions at the lower energies. Normalization at these energies determines an essentially invariant quantity, namely the joint probability for the transferred nucleon being at radius R_1 with respect to the first core nucleus and radius R_2 with respect to the second, where $R_1 \equiv \alpha[A_1^{1/3}/(A_1^{1/3}+A_2^{1/3})]$ and $R_2 \equiv \alpha[A_2^{1/3}/(A_1^{1/3}+A_2^{1/3})]$, α being the distance of closest approach in a head-on collision averaged between incident and final channels. If specific assumptions are made for the geometrical parameters of the bound states, values can be extracted for the product of spectroscopic factors, $S^{(1)}S^{(2)}$; reasonable geometries lead to values of $S^{(2)}$ very close to those previously obtained from light-ion reactions. Above the barrier, the fits to calculations which use nuclear distorted waves are less satisfactory; for optical potentials which give nearly equivalent elastic scattering, the calculations show moderate ambiguity. We believe the leading uncertainty in our analysis is due to the approximate treatment of recoil.

I. INTRODUCTION

Even before heavy-ion accelerators became available, it was recognized by Breit and his collaborators[1] that nucleon-transfer reactions induced by heavy ions with energies well below the Coulomb barrier should be susceptible to relatively unambiguous theoretical interpretation. The dominance of the Coulomb interaction implies that uncertainties due to specifically nuclear interactions between the projectile and target should be minimized. Further, one should be concerned primarily with the "tail" of the wave function of the transferred nucleon, whose radial form, for a given binding energy and angular momentum, is unaffected by the nuclear potential but whose normalization depends on the spectroscopic factor of the transition and the spatial extent of the shell-model potential.

Previous observations of nucleon transfer to light[2] or intermediate[3] mass nuclei have been analyzed to verify, for such nuclei, the applicability of the distorted-wave Born-approximation (DWBA) theory in the sub-Coulomb regime. But although there have been many studies of transfer involving nuclei heavier than Ca with heavy-ion energies above the Coulomb barrier, only the experiments of Barnett *et al.*[4] with a ^{208}Pb target have explored sub-Coulomb transfer for a nucleus of substantial size.

In the present work, we have measured, near the Coulomb barrier, the backward-angle excitation functions of the $(^{16}O, ^{15}N)$ reaction on ^{88}Sr and ^{140}Ce as well as that of the $(^{18}O, ^{17}O)$ reaction on ^{140}Ce. In so doing we have attempted to answer the following questions: To what extent is the sub-Coulomb DWBA theory an accurate tool for the analysis of heavy-ion transfer reactions on nuclei of appreciable size and charge, and over what range of energies does it appear valid? How does the spectroscopic information derived from these analyses compare with that determined from reactions induced by light projectiles? As the Coulomb barrier is surmounted, can we account for the observed excitation functions by incorporating nuclear distortion into the DWBA calculations in a standard fashion?

The stipulations that the low-lying levels of the final nuclei be relatively well separated and that there exist independent determinations of spectroscopic factors led us to the present choice of targets. The low-lying levels of ^{141}Pr have been previously studied through the $^{140}Ce(^3He, d)^{141}Pr$ reaction and the $^{142}Nd(d, ^3He)^{141}Pr$ reaction by Wildenthal, Newman, and Auble[5] and through the $^{140}Ce(^3He, d)^{141}Pr$ reaction by Jones *et al.*[6] Similarly, the population of levels in ^{89}Y has been investigated through the $^{90}Zr(d, ^3He)^{89}Y$ reaction[7,8] and through the $^{88}Sr(^3He, d)^{89}Y$ reaction.[9,10] In both of these residual nuclei there are levels which show appreciable single-particle strengths with little fractionation. Since ^{141}Ce comprises a closed neutron shell plus one neutron, it is expected to show appreciable single-particle strength in its ground state.

Of the several theories for heavy-ion-induced

transfer reactions,[1,11-14] we have restricted our attention to the DWBA formulation of Buttle and Goldfarb.[11] Three versions have been used: (1) Through a series of simplifying assumptions, the sub-Coulomb cross section may be given in analytic form. (2) A more accurate evaluation of the sub-Coulomb cross section follows from numerical integration of the radial integrals containing Coulomb distorted waves. (3) For projectile energies above the barrier, it is necessary to include nuclear as well as Coulomb distortion. The leading assumptions entering these versions are outlined in Sec. III of this paper and some discussion of the reliability of the approximations is given in Sec. IV. Section II is concerned with experimental matters, Sec. V with the energy dependence below and near the barrier, while Sec. VI is devoted to the extraction of spectroscopic factors. Section VII deals with the analysis of data above the barrier.

II. EXPERIMENTAL METHOD AND RESULTS

The variable energy ^{16}O and ^{18}O beams used in the present experiments were provided by injecting a mixture of hydrogen and water vapor or ^{18}O-enriched water vapor into a direct extraction type ion source. The extracted OH^- ions were accelerated by the University of Washington FN tandem Van de Graaff which could yield analyzed oxygen ions of up to 81.0 MeV. A typical beam current on target for 60-MeV oxygen ions of charge state 6^+ was about 300 nA. Thin targets (15–20 $\mu g/cm^2$) of isotopically pure ^{140}Ce enriched to 98.7% and ^{88}Sr enriched to 99.8% were used in the present experiment. The reaction products were detected in surface-barrier detectors placed symmetrically with respect to the beam direction at $\theta_{lab} = 170°$. In the angular distribution measurement, six detectors placed at intervals of 10° were used simultaneously. Typical horizontal angular acceptance $\Delta\theta$ and solid angle $d\Omega$ were 2.9° and 2.13 msr, respectively, at $\theta_{lab} = 170°$. This comparatively large horizontal angular acceptance did not affect the energy resolution appreciably because of the small kinematic broadening at these extreme backward angles (typically less than 15 keV/deg).

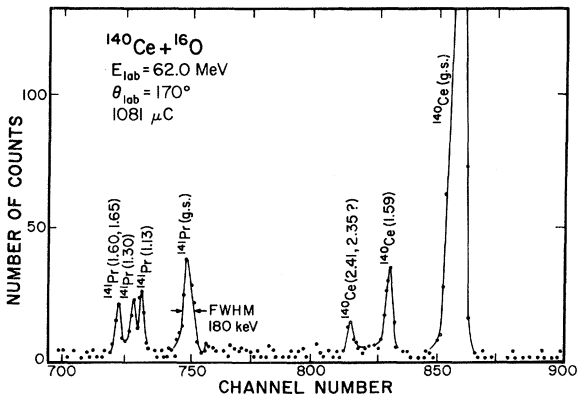

FIG. 1. Backward-angle energy spectrum of outgoing heavy ions for the case $^{140}Ce + ^{16}O$ at $E_{lab} = 62.0$ MeV. Elastic and inelastic scattering and proton transfer to ^{141}Pr are indicated by appropriate designations above the peaks.

Energy spectra of all the heavy ions stopped in the detectors were analyzed to determine peak positions and identities. Peak identities were mainly determined from kinematic considerations which were sufficiently unambiguous in most cases. However, for the $^{140}Ce(^{16}O, ^{15}N)^{141}Pr$ reaction, a standard particle identification technique (with a telescope consisting of an 11-μm-thick ΔE detector, an 87-μm-thick E detector, and a 2-mm-thick antidetector) was employed for added confirmation of the results.

A. $^{140}Ce(^{16}O, ^{15}N)^{141}Pr$ Reaction

A typical energy spectrum taken at $E_{lab} = 62.0$ MeV and $\theta_{lab} = 170°$ is shown in Fig. 1. By a care-

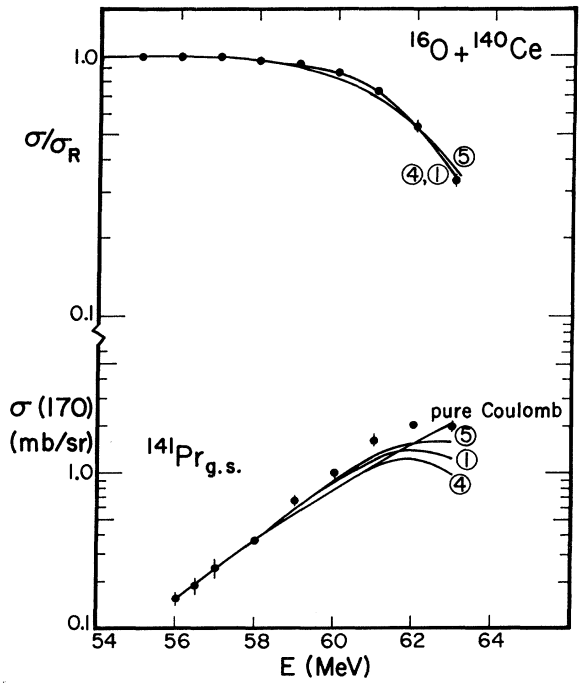

FIG. 2. Elastic excitation functions at $\theta_{lab} = 170°$ for $^{140}Ce + ^{16}O$ and excitation function for proton transfer to the ground state of ^{141}Pr. The numbers 1, 4, and 5 correspond to the "standard" and two other nearly equivalent optical potentials described in text and listed in Table III. The curve labeled "pure Coulomb" corresponds to the sub-Coulomb theory of Buttle and Goldfarb with pure Coulomb waves in the entrance and exit channels.

ful energy calibration employing elastic scattering of ^{16}O ions at different incident energies, the kinematic positions of all the transfer peaks were determined. The ground state of ^{141}Pr ($\frac{5}{2}^+$) was excited most prominently while there was no indication of the first excited state at 0.145 MeV. The levels at 1.13 MeV ($\frac{11}{2}^-$) and 1.30 MeV ($\frac{1}{2}^+$) were not resolved at all energies and the levels at 1.60 MeV ($\frac{3}{2}^+$) and 1.65 MeV ($\frac{1}{2}^+$) could not be resolved at any energy. The only contaminant peak was due to elastic scattering from ^{181}Ta of which there was a very small trace in the target. None of the observed transfer peaks kinematically corresponded to any elastic or transfer peaks in ^{181}Ta. A typical value for the energy resolution was 180 keV [full width at half maximum (FWHM)] as indicated for the peak corresponding to $^{141}Pr_{g.s.}$

Absolute cross sections were obtained by comparing measurements of the ratio of elastic to Rutherford cross section with the ratio of the area under the peak in question to the area under the elastic peak at that energy; at the lowest incident energies, the elastic cross section was assumed to equal the Rutherford value. In Fig. 2, the excitation functions for elastic scattering and transfer to the ground state of ^{141}Pr in the energy range

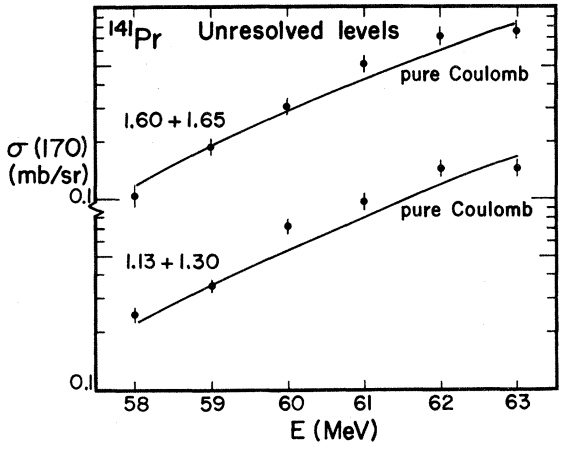

FIG. 3. Excitation functions at $\theta_{lab} = 170°$ for proton transfer to the partially resolved levels at 1.13 and 1.30 MeV and to the unresolved levels at 1.60- and 1.65-MeV states in ^{141}Pr. The curves correspond to the sub-Coulomb theory of Buttle and Goldfarb with no nuclear distortion in the entrance and exit channels. Spectroscopic factors quoted in Table II (obtained from the resolved peaks at $E_{lab} = 59.0$ MeV) were used to calculate the curve labeled 1.13 +1.30. For the curve labeled 1.60 +1.65, the calculation assumed the same relative strength as that quoted by Wildenthal, Newman, and Auble (Ref. 5), $S_{1.60}/S_{1.65} = 1.23/0.54$, and theory was normalized to experiment at $E_{lab} = 59.0$ MeV. The corresponding spectroscopic factors are then $S_{1.60} = 1.50$ and $S_{1.65} = 0.66$.

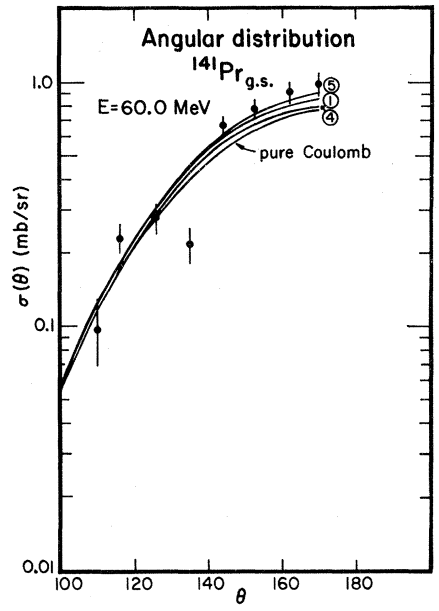

FIG. 4. Angular distribution at $E_{lab} = 60.0$ MeV for the proton transfer to the ground state of ^{141}Pr. The numbers 1, 4, and 5 have the same significance as in Fig. 2 and Table III.

$E_{lab} = 56.0$–63.0 MeV are shown. In Fig. 3 are shown the transfer cross sections to the two sets of unresolved or incompletely resolved levels in ^{141}Pr.

The yields for the other single-nucleon-transfer reactions (^{16}O, ^{15}O), (^{16}O, ^{17}O), and (^{16}O, ^{17}F) were too low to show above the background in our studies. This seems to be consistent with the expectation based on Q-value arguments[15] that proton transfer involving the lighter donor nucleus and heavier acceptor nucleus is here more favored.

In addition, an angular distribution was mea-

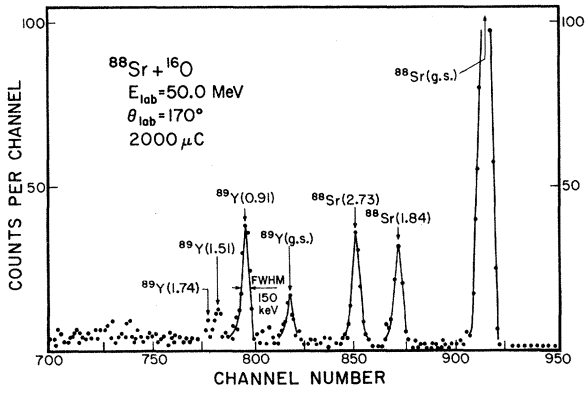

FIG. 5. Backward-angle energy spectrum of outgoing heavy ions for the case $^{88}Sr + ^{16}O$ at $E_{lab} = 50.0$ MeV. Elastic, inelastic, and proton-transfer peaks to ^{89}Y are indicated by appropriate designations above the peaks.

sured at $E_{lab} = 60.0$ MeV for the ground-state proton transfer. The result is shown in Fig. 4.

B. $^{88}Sr(^{16}O,^{15}N)^{89}Y$ Reaction

An energy spectrum taken at $E_{lab} = 50.0$ MeV and $\theta_{lab} = 170°$ is depicted in Fig. 5. The transfer peaks correspond to the $(^{16}O, ^{15}N)$ reaction leading to the ground state $(\frac{1}{2}^-)$, as well as the 0.91- $(\frac{9}{2}^+)$, 1.51- $(\frac{3}{2}^-)$, and 1.74-MeV $(\frac{5}{2}^-)$ states of ^{89}Y. At lower incident energies, the 1.51- and 1.74-MeV states could not be resolved. A typical value for the energy resolution was about 150 keV (FWHM) and was mainly attributable to energy loss in the target. The elastic and transfer excitation functions in the energy range $E_{lab} = 42.5$–50.0 MeV in the present case are plotted in Figs. 6 and 7.

C. $^{140}Ce(^{18}O,^{17}O)^{141}Ce$ Reaction

The elastic excitation function and the excitation function for the neutron transfer to the ground state of ^{141}Ce $(\frac{7}{2}^-)$ in the energy range $E_{lab} = 56.0$ to 61.0 MeV are shown in Fig. 8. The peak areas for this reaction, which were not entirely resolved from inelastic scattering to the first excited states of both ^{18}O and ^{140}Ce, were obtained by a

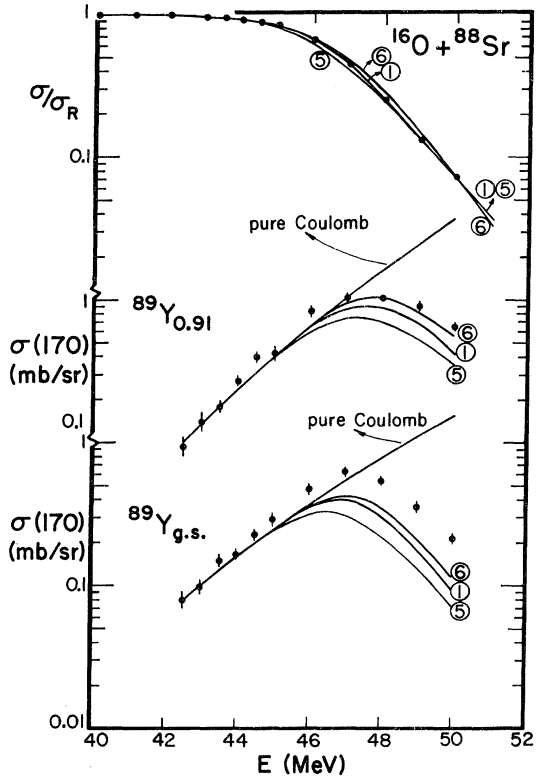

FIG. 6. Elastic excitation function at $\theta_{lab} = 170°$ for $^{88}Sr + ^{16}O$ and excitation functions for proton transfer to the ground state and 0.91-MeV state in ^{89}Y. The numbers 1, 5, and 6 correspond to the "standard" and two other nearly equivalent optical potentials described in text and listed in Table III. The curves labeled "pure Coulomb" correspond to the sub-Coulomb theory of Buttle and Goldfarb with pure Coulomb waves in the incident and exit channels.

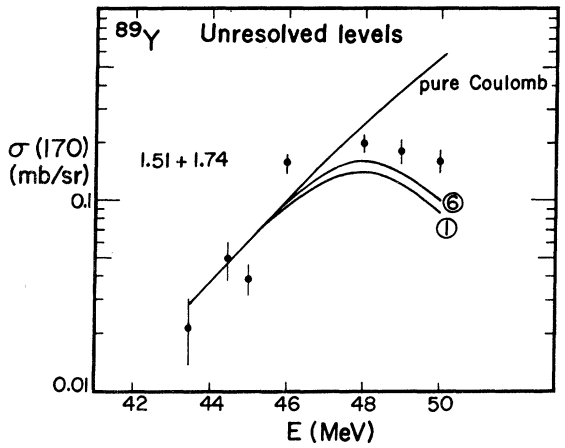

FIG. 7. Excitation function at $\theta_{lab} = 170°$ for the unresolved levels at 1.51 and 1.74 MeV in ^{89}Y. The curves labeled "pure Coulomb," 1 and 6 have the same significance as in Fig. 6. The calculation assumed the same relative strength as that wuoted by Picard and Bassani (Ref. 9), $S_{1.51}/S_{1.74} = 0.11/0.091$, and theory was normalized to experiment at $E_{lab} = 44.5$ MeV. The corresponding spectroscopic factors are then $S_{1.51} = 0.18$ and $S_{1.74} = 0.15$.

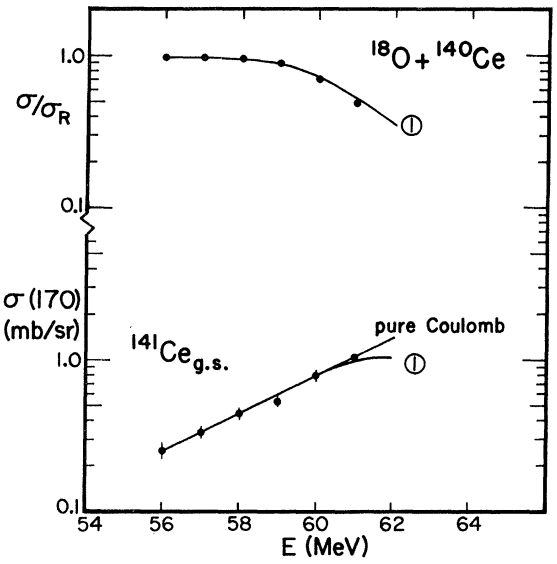

FIG. 8. Elastic excitation function at $\theta_{lab} = 170°$ for $^{140}Ce + ^{18}O$ and excitation function for neutron transfer to the ground state of ^{141}Ce. The curve labeled "pure Coulomb" has the same significance as in other figures and the curve denoted by No. 1 corresponds to the calculations with the "standard" optical-potential parameters for this system listed in Table III.

careful Gaussian peaks least-squares-fitting analysis.

The errors on the experimental points in Figs. 2–4 amd 6–8 are due to the purely statistical uncertainties of our analyses and the curves in these figures represent theoretical calculations which will be discussed in Sec. IV.

III. DWBA THEORY

We briefly discuss the theory of nucleon transfer, following the procedures of Buttle and Goldfarb,[11,15] in order to make explicit both the approximations which are invoked and the various factors which comprise the cross section. Consider a nuclear reaction of the form

$$(c_1+t)+c_2 \rightarrow (c_2+t)+c_1 , \tag{3.1}$$

where c_1 and c_2 are cores between which a nucleon t is transferred. Let l_1, j_1, B_1 and l_2, j_2, B_2 be the orbital angular momenta, total angular momenta, and separation energies of t in the system $(c_1+t) \equiv a_1$ and $(c_2+t) \equiv a_2$, respectively. $\vec{r}$ is the relative coordinate between the two cores, $\vec{r}_1$ and $\vec{r}$ are the coordinates of t with respect to cores c_1 and c_2, respectively, while $\vec{r}_i$ is the relative coordinate between c_2 and a_1 and $\vec{r}_f$ is that between a_2 and c_1

In the post representation, the DWBA matrix element can be written as

$$T_{\mathrm{DWBA}} = \langle \Psi_f^{(-)} | \Delta V_f | \Psi_i^{(+)} \rangle . \tag{3.2}$$

Here $\Psi_f^{(-)}$ and $\Psi_i^{(+)}$ represent products of the distorted waves and the internal wave functions in the final and incident channels and ΔV_f is the difference between the true interaction between the final separated nuclei (c_1 and a_2) and the distorting potential in this final channel. A standard approximation for ΔV_f is that it equals $V_{c_1 t}(\vec{r}_1)$, the shell-model potential of t in c_1; to obtain this form, it is assumed that the difference between the nuclear optical potential, $U_f^{\mathrm{opt}}(r_f)$, and the true interaction between the cores, $V_{c_1 c_2}(r)$, is negligible for those values of core separation, r, which contribute crucially to the integral, and further, that certain Coulomb correction terms may be neglected.[11]

Let us now specialize to situations of sub-Coulomb transfer. By assumption, the distorted waves are represented as pure Coulomb waves and also our neglect above of the difference $(U_f^{\mathrm{opt}} - V_{c_1 c_2})$ is now justified. Further, only the asymptotic form for the radial wave function of t bound to c_2, $u_{l_2}(r_2)$, is expected to contribute appreciably to the integral; thus when t is a neutron, we use the approximation

$$u_{l_2}(r_2) \simeq N_2 h_{l_2}^{(1)}(i\chi_2 r_2), \tag{3.3}$$

where N_2 is the normalization constant, $h_{l_2}^{(1)}$ is a spherical Hankel function of the first kind, and $\chi_2 = (2M_t B_2/\hbar^2)^{1/2}$. When t is a proton, Eq. (3.3) may still be a good approximation to the asymptotic wave function, albeit within a more restricted range of values for r_2, if χ_2 and N_2 are treated as adjustable parameters, χ_2^{eff} and N_2^{eff}.

An additional approximation concerns the relative coordinates of the two nuclei in the incident and final channels,

$$\vec{r}_i = \vec{r} - \frac{M_t}{M_{a_1}} \vec{r}_1$$

and

$$\vec{r}_f = \frac{M_{c_2}}{M_{a_2}} \vec{r} + \frac{M_t}{M_{a_2}} \vec{r}_1 .$$

In the commonly adopted no-recoil approximation, one merely drops the term proportional to $\vec{r}_1$ in these expressions. Buttle and Goldfarb have shown, however, that the no-recoil approximation can result in large discrepancies between DWBA calculations in the post and prior representations, a manifestly undesirable state of affairs. Fortunately, an easily applied approximate correction for recoil often removes much of this post-prior discrepancy.[15] In the post representation, this involves the substitution

$$\vec{r}_i \simeq \vec{r}\left(1 - \frac{M_t}{M_{a_1}} \frac{R_1'}{\alpha}\right), \quad \vec{r}_f \simeq \vec{r}\left(\frac{M_{c_2}}{M_{a_2}} + \frac{M_t}{M_{a_2}} \frac{R_1'}{\alpha}\right). \tag{3.4a}$$

This can be translated into a modification of the wave numbers k_i and k_f since the Coulomb wave functions depend on the products $k_i r_i$ and $k_f r_f$:

$$k_i' = \left(1 - \frac{M_t}{M_{a_1}} \frac{R_1'}{\alpha}\right) k_i , \quad k_f' = \left(\frac{M_{c_2}}{M_{a_2}} + \frac{M_t}{M_{a_2}} \frac{R_1'}{\alpha}\right) k_f . \tag{3.4b}$$

Here R_1' is the radius of a_1 and α is the average of the classical distances of closest approach in the entrance and exit channels in a head-on collision. In all of our calculations where we make comparison to experiment, we shall adopt the above approximate correction for recoil.

The merit of Eq. (3.3) is that it permits use of a powerful addition theorem by which the wave function in $\vec{r}_2$ is to be expressed as a sum of products in $\vec{r}$ and $\vec{r}_1$. Combining this with either the no-recoil approximation or the approximate recoil correction, Eqs. (3.4), enables one to reduce the original six-dimensional DWBA integral to products of two three-dimensional integrals, one of which has the familiar form of the conventional zero-range approximation. The differential cross section for the sub-Coulomb transfer reaction, incorporating the approximate correction for re-

coil can then be written as

$$\left(\frac{d\sigma}{d\Omega}\right) = 4\pi \frac{M_i M_f}{(2\pi\hbar^2)^2} \frac{k_f}{k_i} \left(\frac{2J_{a_2}+1}{2J_{c_2}+1}\right) \frac{S^{(1)}S^{(2)}}{(2j_2+1)} |A_{l_1}|^2 [N_2^{\text{eff}}]^2$$

$$\times \sum_{l\lambda} \langle j_1 \tfrac{1}{2} l 0 | j_2 \tfrac{1}{2} \rangle^2 |T_{l\lambda}(\theta)|^2, \quad (3.5)$$

where

$$T_{l\lambda}(\theta) = \int d\vec{r}\, \chi_f^{(-)*}(\vec{k}_f', \vec{r}) h_l^{(1)*}(i\chi_2^{\text{eff}} r) Y_{l\lambda}^*(\hat{r}) \chi_i^{(+)}(\vec{k}_i', \vec{r}), \quad (3.6)$$

$$A_{l_1} = \int_0^\infty r_1^2 dr_1 j_{l_1}^*(i\chi_2^{\text{eff}} r_1) V_{c_1 t}(r_1) u_{l_1}(r_1). \quad (3.7)$$

M_i, M_f are the reduced masses in entrance and exit channels, k_i, k_f are the momenta in entrance and exit channels, k_i', k_f' are the recoil corrected momenta as defined in Eq. (3.4b), J_{a_2}, J_{c_2} are the total angular momenta of a_2 and c_2, $S^{(1)}$, $S^{(2)}$ are the spectroscopic factors of t in a_1 and a_2, and l is the transferred orbital angular momentum.

The most accurate evaluation of the integral $T_{l\lambda}(\theta)$ is accomplished through numerical integration using a large computer; in our calculations we have used a version of the computer code DWUCK[16] which allows a maximum of 100 partial waves to compute $T_{l\lambda}(\theta)$.

Use of a large computer may be circumvented, however, since a simple analytic expression for the cross section can be derived[15] on making three further assumptions: (1) For values of r near the classical turning points of the heavy-ion trajectories, the function $h_l^{(1)}(i\chi_2 r)$ is reasonably well approximated by

$$h_l^{(1)}(i\chi_2 r) \simeq f h_0^{(1)}(i\chi r), \quad (3.8)$$

where f and χ are adjustable parameters. (2) The angular-dependent term in the form factor, $Y_{l\lambda}^*(\hat{r})$ can be replaced by $Y_{l\lambda}^*(\hat{R})$, where $\hat{R}$ denotes the recoil direction along which the contribution to the integral Eq. (3.6) is a maximum. (3) The Coulomb parameters in the incident and final channels, η_i and η_f, are much larger than unity. With these assumptions, the sum in Eq. (3.5) can be shown to reduce to a simple analytical expression [Eqs. (2.11), (2.13), (2.15), and (2.16) of Ref. 15 with, however, the small modification that k_i in these equations should be replaced by k_i'], which can be easily calculated. The accuracy of this analytic expression will be considered in the next section.

If the heavy ions surmount the Coulomb barriers in either the incident or final channel, a number of approximations made in deriving Eq. (3.5) become suspect. Certainly, pure Coulomb waves are no longer correct for the distorted waves. Also, it is no longer clear that the asymptotic form is appropriate for the wave function $u_{l_2}(r_2)$, that the difference $(U_f^{\text{opt}} - V_{c_1 c_2})$ in the form factor may be neglected, or that the approximate recoil correction is valid. In this paper, though, we shall adopt an optimistic attitude: The only modification we make as the barrier is surmounted is to use wave functions distorted by a complex nuclear potential as well as by the Coulomb interaction. As is typical in such applications, these distorted wave functions will be chosen to give a good account of the elastic excitation functions.

IV. RELIABILITY OF APPROXIMATIONS

We first examine the validity of Eq. (3.3) according to which the wave function $u_{l_2}(r_2)$ is approximated by a Hankel function in the region of interest; since we are primarily concerned with proton transfer reactions, it is by no means obvious that such a replacement is well justified there.

Codes have been constructed[17] for full finite-range calculations with neglect of recoil in which one attempts to evaluate the six-dimensional DWBA integral for all values of r_2. There are

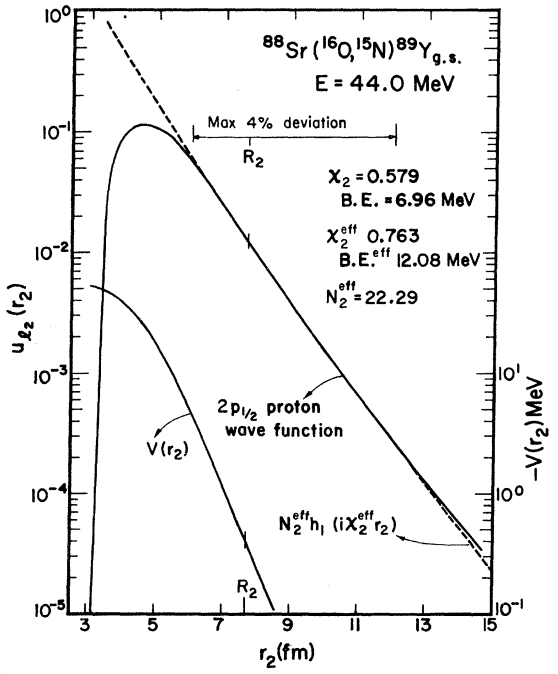

FIG. 9. The Hankel function approximation to the $2p_{1/2}$ ground-state proton radial wave function in ^{89}Y. The match center radius R_2 equals 7.7 fm at E_{lab} = 44 MeV. The significance of $\chi_2, \chi_2^{\text{eff}}$ and N_2^{eff} is described in text. $V(r_2)$ is the nuclear potential appropriate to this bound state with r_{02} = 1.2 fm and a_2 = 0.65 fm. It is clear that R_2 is well outside the nuclear potential. In fact, at R_2 = 7.7 fm, $-V(R_2) \simeq$ 0.4 MeV compared to the central depth of 59.7 MeV.

indications,[18] however, that the cross sections so computed do not differ appreciably from those which make use of the above Hankel function approximation. Our belief is that there are other approximations in our procedure which have more doubtful validity.

A least-squares-fitting routine optimizes the fit around a "match center" radius in the second potential, R_2, defined as $[A_2^{1/3}/(A_1^{1/3}+A_2^{1/3})]\,\alpha$, where α is the distance of closest approach for a head-on Coulomb collision averaged between the incident and exit channels referred to in Eq. (3.4). In Fig. 9 is shown a fit to the ground-state proton orbital of ^{89}Y for which the radius parameter of the potential is chosen to be 1.20 fm. It is seen that a good fit is achieved over a rather broad range of r_2; with a match center radius R_2, at 7.7 fm (corresponding to an incident laboratory energy of 44 MeV) the deviation exceeds 4% only for r_2 less than 6 fm or greater than 12 fm. As long as α comfortably exceeds the sum of the radii of the potential wells, it is not expected that $u_{l_2}(r_2)$ will contribute much to the matrix element for values of $r_2 < R_2'$, where $R_2' = 1.2A_2^{1/3}$, here approximately equal to 5.5 fm.

If the DWBA amplitude is computed in the prior rather than the post representation, the roles of projectile and target are exchanged. Consequently, for our proton-transfer reactions, the coordinate r_2 is then that of the proton relative to the ^{15}N core. In Fig. 10 is displayed the $1p_{1/2}$ proton wave function in ^{16}O and the corresponding Hankel function approximation. The match center radius 4.3 fm corresponds to the same reaction as in Fig. 9, i.e., ^{88}Sr(^{16}O, ^{15}N)^{89}Y$_{g.s.}$, at an incident laboratory energy of 44 MeV. Again, it is seen that the Hankel function approximation is rather accurate.

The extent to which contributions to the transfer amplitude are localized near the classical distance of closest approach is illustrated in Fig. 11 which shows the factors comprising a radial matrix element for the reaction ^{88}Sr(^{16}O, ^{15}N)^{89}Y$_{g.s.}$. We see that the region of transfer is localized within 3 fm in this instance, a result which implies that the wave function $u_{l_2}(r_2)$ need be matched only over a limited region. Also we have found in further numerical studies that shifting the match center radius R_2 by as much as 1 fm alters the calculated cross section by less than 1%.

In the calculations discussed so far, a reasonable but arbitrary value was adopted for the radius parameter of the shell-model potential. One may then worry as to what extent this choice affects the cross sections through altering the values determined for χ_2^{eff}. Fortunately, this dependence appears to be rather small; keeping the magnitudes $S^{(2)}\,|\,u_{l_2}(r_2=R_2)|^2$ constant at the match center radius, we find that for values of r_{02} ranging

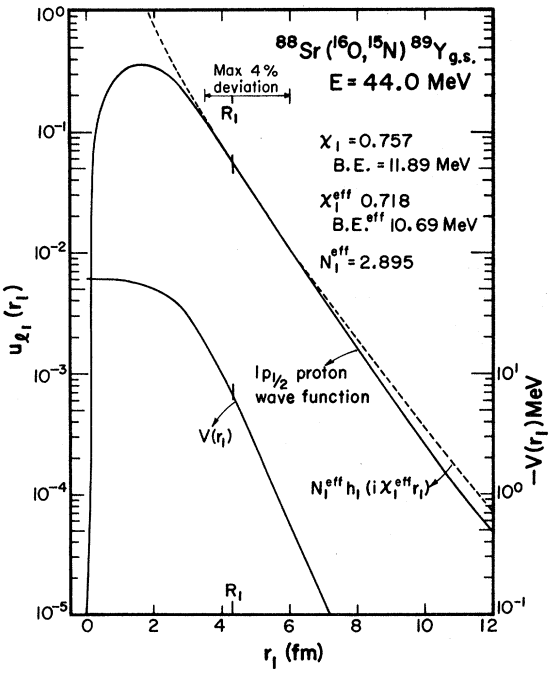

FIG. 10 The Hankel function approximation to the $1p_{1/2}$ ground-state proton radial wave function in ^{16}O. R_1, χ_1, χ_1^{eff}, and N_1^{eff} correspond now to the appropriate prior calculations.

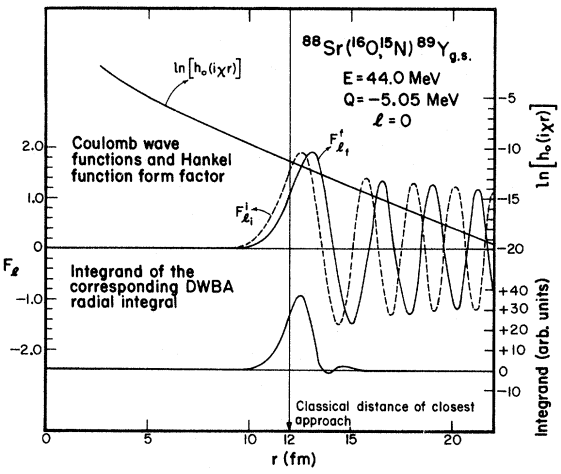

FIG. 11. Localization of transfer for the $l=0$ proton transfer to the ground state of ^{89}Y at $E_{\text{lab}}=44$ MeV. The Coulomb wave functions in the entrance and exit channels for $l_i = l_f = 2$, corresponding to the classical grazing angular momentum at $\theta_{\text{lab}} = 170°$, the natural logarithm of the Hankel function form factor and the product $F_{l_f} \times h_0^{(1)}(i\chi r) F_{l_i}$ which is proportional to the integrand of the radial DWBA integral are ahown, as a function of distance between the colliding nuclei. The latter curve clearly indicates that the main contribution to the cross section is centered around the classical distance of closest approach with a spread of about 3 fm.

from 1.14 to 1.26 fm, the calculated cross section at 170° for the reaction $^{88}Sr(^{16}O, ^{15}N)^{89}Y_{g.s.}$ at an incident energy of 44 MeV is constant to within 0.5%. Similarly for values of r_{02} ranging from 1.18 to 1.30 fm the cross section at 170° for the reaction $^{140}Ce(^{16}O, ^{15}N)^{141}Pr_{g.s.}$ at an incident energy of 55 MeV is constant to within 3%. In addition, a 5% variation in the diffuseness parameter a_2 about its "standard" value 0.65 fm produced variations in cross section less than 2%. We shall return to some implications of these results in Sec. VI where we discuss spectroscopic factors.

Next, we examine our neglect of the Coulomb correction terms contained in ΔV_f. These have the form,[11] in the post representation,

$$\Delta V_{\text{Coul}} = Z_1 Z_t e^2 r_1^{-1} + Z_1 Z_2 e^2 r^{-1} - Z_1(Z_2 + Z_t)e^2 r_f^{-1} \tag{4.1}$$

$$= Z_1 Z_t e^2 (r_1^{-1} - r^{-1}) + Z_1(Z_2 + Z_t)e^2(r^{-1} - r_f^{-1}) \tag{4.2}$$

and for grazing collisions are well approximated by

$$\Delta V_{\text{Coul}} = Z_1 Z_t e^2 (r_1^{-1} - r^{-1}) - Z_1(Z_2 + Z_t)e^2 M_t M_{c_2}^{-1} r_1 r^{-1} \times (r_1^{-1} - M_{a_2} M_{c_2}^{-1} r^{-1}). \tag{4.3}$$

As was found by Buttle and Goldfarb[11] for the $^{10}B(^{14}N, ^{13}C)^{11}C$ reaction, inclusion of the Coulomb correction terms decreases the form factor at all values of r for proton stripping reactions. A similar inclusion of Coulomb correction terms increases it slightly for neutron stripping reactions. Quantitatively this amounted to approximately 30% reduction for the $(^{16}O, ^{15}N)$ reactions and about 8% increase for the $(^{18}O, ^{17}O)$ reaction over the Coulomb-uncorrected cross sections. The relative difference between the form factors which enter Eq. (3.6) with and without the Coulomb correction terms varies only slowly with distance between cores, r; for example, in the case of proton transfer to the ground state of ^{89}Y using post representation at $E = 44$ MeV, the ratio of the difference of form factors to the form factor without the Coulomb terms is 0.146 at $r = 10.5$ fm and 0.175 at $r = 12.5$ fm.

Numerical evaluation of the transfer cross sections with inclusion of Coulomb correction terms has been made with the aid of the computer code DWUCK for all levels under the present study for the lowest bombarding energies. In addition, for the ground state and 0.91-MeV state in ^{89}Y, the energy variation of the Coulomb corrections was also investigated and the latter results are shown in Table I; in these calculations nuclear distortions are not included. The relative angular distributions are rather insensitive to inclusion of these terms and inspection of Table I shows that the decrease in cross section is only slightly dependent on energy and l transfer. Similarly, the relative reduction was found to be essentially the same when, at higher energies, nuclear distorted waves were used. In view of this and the non-negligible expense of carrying out computations at all energies of interest, the detailed excitation functions shown in this paper do not include the Coulomb correction terms. However, when we later relate the geometry of the bound states and their spectroscopic factors to the magnitude of our measured cross section, we will take account of the corrections due to Coulomb terms.

We next discuss the validity of the no-recoil approximation and the approximate recoil correction of Buttle and Goldfarb. At this time of writing, DWBA computations which treat recoil exactly[19] are not yet available for collisions of heavy ions with nuclei as heavy as those we are considering and consequently a direct check of our recoil approximations has not been made. However, a necessary condition which must be placed on the exact DWBA amplitude—that it be the same for either the post or prior representation—may be used as a measure of the consistency of the recoil approximations. Here we find, as did Barnett *et al.*[4] for the case of transfer reactions on ^{208}Pb,

TABLE I. Effect of Coulomb terms in the form factor.

	$^{89}Y_{g.s.}$ $\sigma(170)$ [a] (mb/sr)			$^{89}Y_{0.91}$ $\sigma(170)$ [a] (mb/sr)		
E (MeV)	with Coulomb terms	without Coulomb terms	Fractional deviation	with Coulomb terms	without Coulomb terms	Fractional deviation
44	0.129	0.188	0.31	0.290	0.412	0.30
46	0.308	0.439	0.30	0.827	1.158	0.29
48	0.659	0.929	0.29	2.085	2.879	0.28
50	1.285	1.809	0.29	4.733	6.439	0.27

[a] These calculations assumed "standard" bound-state geometries with $S^{(1)} = 2.0$ and $S^{(2)} = 1.0$.

that the post and prior cross sections are generally in closer accord when the approximate recoil correction is made than when the no-recoil approximation is used. Accordingly for theoretical calculations which involve fits with experimental data, we have used the approximate recoil corrections.

However, it is only fair to point out that in some cases [(e.g., ^{88}Sr(^{16}O, ^{15}N)^{89}Y$_{g.s.}$)] for the physical Q values and energies of interest, the post-prior discrepancy for the no-recoil approximation is no worse than that with the approximate recoil correction. Figure 12 illustrates this point. Indeed, one sees in Fig. 12 that the discrepancy when the no-recoil approximation is used may actually be less over a considerable range of incident energies. But this region, in the present case, lies above the region where sub-Coulomb calculations may be considered legitimate. In addition, it is evident from Fig. 12 that when the Coulomb terms are also included in the form factor, post and prior results agree better than when they are neglected.

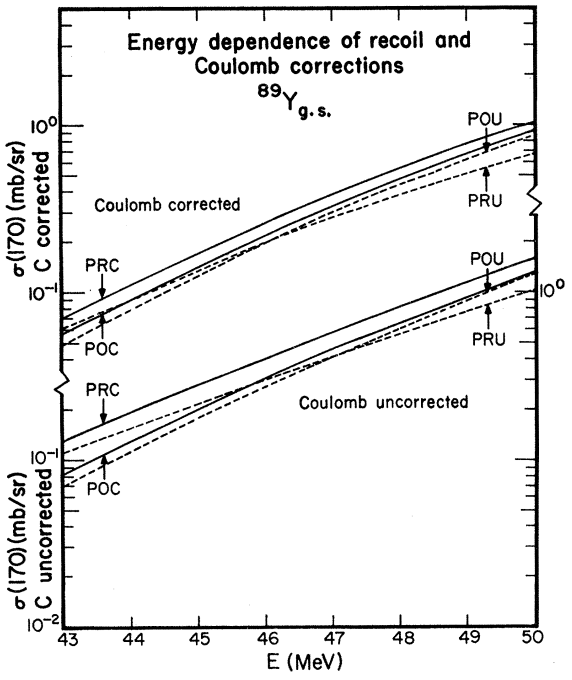

FIG. 12. The effects of Coulomb corrections in the form factor and recoil corrections in the entrance and exit channel wave functions for post and prior representations, as a function of incident energy. The specific case is that of proton transfer to ^{89}Y$_{g.s.}$ at $\theta_{lab}=170°$. No nuclear distortion is introduced and the calculations assume $S^{(1)}=2.0$ and $S^{(2)}=1.0$. The symbols POC and POU correspond to the calculations with and without recoil corrections, respectively, in the post representation. Similarly, PRC and PRU are the recoil corrected and uncorrected calculations in the prior representation. The top part of the figure depicts calculations which assume Coulomb correction in the form factor, while the bottom part shows those that do not.

Buttle and Goldfarb[15] have argued that the post representation is to be preferred if the Q value is negative and if the light nucleus is the donor of the transferred particle. Accordingly, the post representation should be favored for the transfer reactions we are considering. Nonetheless, the discrepancies that are apparent in Fig. 12 do give us pause and lead us to regard our approximate treatment of recoil as the least satisfactory aspect of our calculations. As pointed out by DeVries and Kubo[19] and by Nagarajan,[20] a less approximate handling of recoil leads to modified selection rules for orbital angular momentum transfer giving rise, in some cases, to large changes in the magnitudes of the calculated cross sections.

The simple analytic approximation[15] for the DWBA cross section appears to be rather good, particularly for low values of the angular momentum transfer. For example, for the $l=0$ proton transfer to the ground state of ^{89}Y, the two cross sections at 170° agree to within 3%, and even for the $l=5$ proton transfer to the 0.91-MeV first excited state of ^{89}Y, the agreement was within 4% at 170° for incident energies from 42 to 47 MeV. The largest deviation, about 15%, occurred for the $l=6$ proton transfer to the $1h_{11/2}$ state at 1.13 MeV in ^{141}Pr. Thus the simple analytic approximation seems to be somewhat more accurate for the cases we have examined than was found by Barnett *et al.*[4] and has been very useful for studying the dependence of the cross sections on various parameters and approximations.

Parenthetically, we mention that the DWBA cross sections, as computed with the code DWUCK, settled down to a constant value at a relatively low value for l_{max}, the maximum number of partial waves. This is to be contrasted to the experience of Barnett *et al.*[4] For example, at the backward angle of 170°, we find the difference between the proton-transfer cross sections with $l_{max}=56$ and $l_{max}=100$ to be always less than 0.5% for the proton transfer to the ground state of ^{89}Y. For all the cases that we have studied, $l_{max}\leq 72$ was found to be sufficiently accurate (i.e., there is less than 1% variation in backward-angle cross section for values of l_{max} larger than approximately 70).

V. ENERGY DEPENDENCE BELOW AND NEAR THE COULOMB BARRIER

In Figs. 2, 6, and 8, the excitation functions to single levels, measured at 170°, are compared to theoretical sub-Coulomb cross sections (which neglect the Coulomb correction terms in the form

factor) Eq. (3.5), evaluated with a modified form of the computer code DWUCK. The calculated cross sections have been normalized to experimental results at low values of bombarding energy.

We see that the measured and calculated cross sections are in accord over a substantial range of bombarding energies, giving us some evidence that the sub-Coulomb theory is appropriate at our lower energies. Somewhat surprisingly, the agreement persists even to energies where the elastic scattering lies substantially below the Rutherford value. As mentioned in the previous section, the cross sections which include the Coulomb correction terms have, for all practical purposes, the same energy dependence as those that do not.

To determine at what energies we should expect to encounter deviations from the sub-Coulomb theory, the elastic scattering excitation functions have been fitted to optical-model calculations which employ a standard four-parameter complex Woods-Saxon potential and the transfer cross sections have been recomputed using waves distorted by this nuclear potential as well as the Coulomb potential. Obviously, the information content in the backward-angle elastic excitation functions is rather low so that a variety of potential parameters are possible. A full discussion of alterations in the computed transfer cross sections produced by nuclear distortion is deferred to Sec. VII. We here note, however, than any reasonable distorting potential we have examined leads to negligible changes in cross sections for $E_{\rm lab}<58$ MeV for proton transfer to states in ^{141}Pr, for $E_{\rm lab}<45$ MeV for proton transfer to states in ^{89}Y, and for $E_{\rm lab}<60$ MeV for the neutron transfer to the ground state of ^{141}Ce. At these energies, the elastic cross sections are diminished from the appropriate Rutherford value by 5%, 15%, and 30%, respectively. The classical barrier presented by the real part of the nuclear potential and the Coulomb potential[21] occurs at $E_{\rm lab}=62.8$ MeV and $r_b\simeq 11.3$ fm for ^{16}O + ^{140}Ce, $E_{\rm lab}=47.1$ MeV and $r_b\simeq 10.5$ fm for ^{16}O + ^{88}Sr, and $E_{\rm lab}=61.9$ MeV and $r_b=11.6$ fm for ^{18}O + ^{140}Ce.

VI. SPECTROSCOPIC FACTORS

Unambiguous extraction of spectroscopic factors for the target nucleus is an exceedingly difficult goal since this requires not only that the sum $\sum_\lambda |T_{l\lambda}(\theta)|^2$ be accurately evaluated, but also that one know the spectroscopic factor of the projectile and the geometry of both bound states. Accordingly, we postpone the discussion of our best estimates for such spectroscopic factors to a later portion of this section.

We do find, however, one invariant quantity, a function of spectroscopic factors and well geometries, which fixes the over-all magnitude of a transfer cross section. At first glance, one might guess that this invariant would be the product occurring in Eq. (3.5), $S^{(1)}S^{(2)}|A_{l_1}|^2[N_2^{\rm eff}]^2$, but numerical studies with many different well geometries show otherwise. The problem with the above product is that small changes in the values of $\chi_2^{\rm eff}$, which occur as the geometrical parameters or bombarding energy are varied, lead to moderately large changes in both $|A_{l_1}|^2$ and $[N_2^{\rm eff}]^2$. But, as noted earlier in Sec. IV, these are compensated for by changes in $\sum_\lambda |T_{l\lambda}(\theta)|^2$ which is also a function of $\chi_2^{\rm eff}$, so that the over-all cross section is essentially unchanged provided the magnitude $S^{(2)}|u_{l_2}(r_2=R_2)|^2$ is held fixed. Similarly, it is found that $S^{(1)}|A_{l_1}|^2$ is essentially unchanged when there are changes in the geometrical parameters of the first well provided that $S^{(1)}|u_{l_1}(r_1=R_1)|^2$ is held fixed. To be specific, the value of $S^{(1)}|A_{l_1}|^2$ for proton transfer from ^{16}O to ^{89}Y$_{\rm g.s.}$ at $E_{\rm lab}=44$ MeV varied by less than 1.5% as r_{01} ranged from 1.14 to 1.26 fm and a_1 ranged from 0.56 to 0.64 fm, provided that $S^{(1)}|u_{l_1}(R_1=4.33)|^2$ was held fixed.

Thus our suggested invariant is the joint probability

$$P(R_1,R_2)=S^{(1)}S^{(2)}|u_{l_1}(R_1)|^2|u_{l_2}(R_2)|^2 . \qquad (4.4)$$

That this should be an invariant for sub-Coulomb transfer becomes physically plausible on contemplating the overlap of the radial wave functions when the projectile and target are at the distance of closest approach.

The joint probability $P(R_1,R_2)$ together with the corresponding values of R_1 and R_2 are listed in Table II for those transitions to levels which could be resolved. In obtaining these values, we have used the post form of the sub-Coulomb DWBA theory including the approximate recoil corrections suggested by Buttle and Goldfarb and also have taken into account the Coulomb correction terms in the form factor as discussed in Sec. IV. The normalization to experiment is that shown in Figs. 2–4 and 6–8, and the corresponding incident laboratory energies are also listed in Table II.

In carrying out these calculations, some choice had to be made for the bound-state parameters. Such choices seem to be often based largely on custom rather than any strict theoretical foundation; our own was based on a reasonable sampling from literature. These "standard" bound-state parameters used in the present calculations were $r_{01}=r_{0c}=1.20$ fm, $a_1=0.65$ fm for the nucleon bound to the light-donor nucleus, and $r_{02}=r_{0c}=1.24$ fm, $a_2=0.65$ fm for the nucleon bound to the

TABLE II. Summary of results.

Nucleus	l	Final state	E (MeV)	$P(R_1,R_2)$	R_1 (fm)	R_2 (fm)	$\Lambda^{(1)}\Lambda^{(2)}$	χ_1^{eff}	χ_2^{eff}	$S^{(1)}S^{(2)}$	$S^{(2)}$ [a]
^{141}Pr	3	g.s.	56	2.67×10^{-7}	4.41	9.09	1.31×10^{5}	0.7184	0.7713	1.73	0.81 ± 0.05
	6	1.13	59	4.60×10^{-7}	4.22	8.71	8.01×10^{2}	0.7179	0.7069	2.22	1.04 ± 0.18
	1	1.30	59	1.25×10^{-6}	4.22	8.73	2.87×10^{5}	0.7179	0.7387	1.73	0.81 ± 0.30
^{89}Y	0	g.s.	42.5	7.19×10^{-7}	4.49	7.95	7.26×10^{4}	0.7184	0.7574	2.51	1.17 ± 0.16
	5	0.91	42.5	1.96×10^{-7}	4.56	8.08	4.51×10^{2}	0.7183	0.6872	1.55	0.72 ± 0.09
^{141}Ce	1,3,5	g.s.	56	1.62×10^{-6}	4.63	9.21	1.65×10^{2}	0.5399	0.4848	1.80	1.11 ± 0.08

[a] The errors assigned to $S^{(2)}$ are due to counting statistics only.

heavy-acceptor nucleus. The value of the spin-orbit potential V_{so} was assumed to be 7.0 MeV throughout. But, as emphasized above, the values extracted for $P(R_1,R_2)$ only vary slightly as these range over all reasonable values. Since the joint probability $P(R_1,R_2)$ is a function of R_1 and R_2, it may easily be extrapolated locally to other values of match center radii when use is made of the Hankel function approximation.

For the case of neutron transfer, where the values of χ_2 and χ_1 are determined by the respective binding energies, the specification of $P(R_1,R_2)$ is uniquely related to the product $\Lambda^{(1)}_{l_1j_1}\Lambda^{(2)}_{l_2j_2}$, where Λ_{lj} is the reduced normalization of Rapaport and Kerman,[22] $\Lambda_{lj}=N^2_{lj}S_{lj}/\chi^3$ (superscripts 1 or 2 should be added to refer to cores 1 and 2, respectively). For the case of proton transfer, however, the values of Λ_{lj} are not so uniquely determined for a given proton wave function since the values of χ are functions of the match center radii; consequently, there is modest variation in the values of N^{eff} and thus Λ_{lj} as a function of the bombarding energy at which one chooses to normalize theory to experiment. Similarly, the values of Λ_{lj} are moderate functions of the geometry assumed for the potential wells. For example, the observed proton-transfer cross section to the ground state of ^{89}Y, at $E_{\text{lab}}=44$ MeV and $\theta_{\text{lab}}=170°$, 0.16 mb/sr, leads to a value for the product $\Lambda^{(1)}_{l_1j_1}\Lambda^{(2)}_{l_2j_2}$ with $r_{01}=1.20$ fm and $r_{02}=1.24$ fm which is 18% higher than that for the choice $r_{01}=r_{02}=1.20$ fm; in contrast, the value of $P(R_1,R_2)=P(4.33,\ 7.67)$ is found to be only 2% higher for the choice $r_{01}=1.20$ fm and $r_{02}=1.24$ fm than it is for $r_{01}=r_{02}=1.20$ fm. Bearing in mind the above comments, we nonetheless also list values extracted for the product $\Lambda^{(1)}_{l_1j_1}\Lambda^{(2)}_{l_2j_2}$ and the corresponding values of χ_1^{eff} and χ_2^{eff} in Table II. These values also pertain to the "standard" geometry.

When specific assumptions are made regarding the geometrical parameters of the bound states, as mentioned earlier, values can be extracted for the product of spectroscopic factors $S^{(1)}S^{(2)}$. Choosing the "standard" bound-state parameters mentioned earlier, we obtain the values given in Table II. In addition, a knowledge of $S^{(1)}$ is necessary for the further evaluation of $S^{(2)}$. For this purpose, we have assumed the measured value,[23] $S^{(1)}=2.14$, for the $p_{1/2}$ hole state in ^{16}O (the bound-state geometry used in extracting this is the same as ours) and the calculated value of Kuo and Brown,[24] $S^{(1)}=1.62$ for the $d_{5/2}$ state in ^{18}O.

A comparison of our results on spectroscopic factors with those obtained by other workers using light-ion-induced reactions is often ambiguous due to the nonunique sets of bound-state parameters, normalization constants, use of lower radial cut-offs in some cases, uncertainties in optical parameters in the incident and final channels, and experimental errors quoted by these authors, coupled with our own problems as mentioned in the beginning of this section. Nevertheless, it may be instructive to undertake such a general comparison with the above reservations in mind.

With the same geometry for the bound-state parameters for the ^{140}Ce$+p$ system as ours, Wildenthal, Newman, and Auble[5] obtain spectroscopic factors of 0.64, 0.84, and 0.65 for the ground state, 1.13-MeV, and 1.30-MeV states in ^{141}Pr, respectively, whereas the corresponding values of Jones *et al.*[6] are 0.46, 0.60, and 0.49. These have to be compared with our results which are 0.81, 1.04, and 0.81, respectively. These values show some systematic tendencies. Our results are roughly 25% higher and those of Jones *et al.* are 28% smaller than the corresponding results of Wildenthal, Newman, and Auble.[5] It should be pointed out that the latter authors stress the significance of the relative spectroscopic factors rather than their absolute values, due to normalization problems. Except for the completely unresolved levels at 1.60 and 1.65 MeV in ^{141}Pr (where we have assumed the relative spectroscopic factors of Wildenthal, Newman, and Auble[5]), our derived relative strengths for the resolved states agree with those of Wildenthal, Newman,

and Auble[5] and Jones *et al.*[6]

For the states in ^{89}Y, the comparison becomes more difficult due to the different bound-state parameters used by Picard and Bassani[9] and Stautberg, Kraushaar, and Ridley[10] in their studies of the ^{88}Sr(^{3}He, d)^{89}Y reaction. For the resolved states in ^{89}Y (ground state and the first excited state at 0.91 MeV), the spectroscopic factors extracted from the present experiment (1.17 and 0.72) have to be compared with the values 0.90 and 0.88 of Picard and Bassani[9] and 1.62 and 1.62 of Stautberg, Kraushaar, and Ridley.[10]

A word of caution is in order here. Most of the (^{3}He, d) results that we quoted here have relied heavily on spectroscopic sum rules to extract spectroscopic factors for the various states. This usually involves additional normalization constants which are quite arbitrary. Therefore, even with identical bound-state parameters, a comparison of these absolute spectroscopic factors to ours may have only dubious relevance.

For the neutron-transfer reaction populating the ground state of ^{141}Ce, our value of $S^{(2)}$ is 1.11. The (d, p) reaction study of Wiedner *et al.*[25] yields a value of 0.89. If we adopt their bound-state geometry ($r_{02} = 1.23$ fm, $a_2 = 0.65$ fm), our result becomes 1.15 which makes their result 25% less than ours.

VII. EXCITATION FUNCTIONS ABOVE THE BARRIER

It is apparent from Figs. 2, 6, and 7 that above some critical bombarding energy, the observed excitation functions dip below those calculated from sub-Coulomb theory. Qualitatively, this deviation may be attributed to nuclear distortion as the Coulomb barrier is surmounted.

We have attempted to account quantitatively for this behavior by using wave functions in the entrance and exit channels which are distorted by a complex nuclear potential as well as by the Coulomb potential. "Standard" optical-model parameters which yield reasonable fits to the elastic excitation functions are listed in Table III and calculated transfer cross sections using these parameters are shown in Figs. 2, 4, 6, 7, and 8. Inspection of Figs. 2, 6, and 7 indicates, however, that there are some serious discrepancies between the magnitude of these calculations and experimental results at higher bombarding energies. However, the general trend and the location of the peaks of the excitation functions are reproduced by the present calculations.

TABLE III. Typical sets of optical-model parameters used in the present calculations.

System	V (MeV)	W (MeV)	$r_0 = r_{0c}$ (fm)	a_0 (fm)	Designation in Figs.
^{16}O + ^{140}Ce	80	15	1.250	0.50	1 [a]
	80	15	1.304	0.40	4
	80	15	1.201	0.60	5
^{16}O + ^{88}Sr	40	10	1.310	0.45	1 [a]
	40	10	1.342	0.40	5
	40	10	1.280	0.50	6
^{18}O + ^{140}Ce	80	15	1.250	0.55	1 [a]

[a] These are defined as "standard" parameters in text.

Since the optical parameters are far from uniquely determined by the requirement that the backward-angle elastic excitation functions be fitted, we have also calculated the transfer cross sections to the ground state, 0.91-MeV, 1.51-MeV, and 1.74-MeV states in ^{89}Y and to the ground state of ^{141}Pr, using alternate values of the parameters which gave only slightly inferior fits to the elastic excitation functions. A sampling of these results is labeled by the numbers 4 and 5 on the curves in Fig. 2, and 5 and 6 in Fig. 6. In addition, fits to an experimental angular distribution taken at $E_{lab} = 60$ MeV for ^{141}Pr$_{g.s.}$ (Fig. 4) with these optical potentials indicate that the shapes of the calculated angular distributions are essentially unchanged from the sub-Coulomb calculation, even though the magnitudes at backward angles are altered somewhat.

The general trend of our calculations above the barrier seems to indicate that transfer cross sections are better reproduced by higher diffuseness in the optical potential, even though the corresponding elastic fits got progressively worse. A tendency for the theoretical fits with "standard" parameters to flatten out with respect to the experimental results is evident as shown in Fig. 8 for the elastic scattering of ^{18}O on ^{140}Ce. However, the corresponding transfer cross section to ^{141}Ce$_{g.s.}$ is very well reproduced by the sub-Coulomb theory with no nuclear distortion. In fact, inclusion of optical potentials to distort the incident and final channels has only a minor effect on the transfer cross section as seen by the curve labeled 1 in Fig. 8.

An investigation of the dependence of the elastic and transfer excitation functions on the imaginary part of the optical potential, W, produced some surprising results for low values of the ratio (W/V). For certain combinations of the values of the radius and diffuseness parameters, a small change in the value of W produced only minor changes in the calculated elastic excitation functions, whereas the same change in W sometimes resulted in calculated transfer excitation functions, which wildly oscillated at higher incident energies. For example, for the ^{16}O + ^{88}Sr system, with the

set of optical parameters $r_0 = 1.31$ fm, $a_0 = 0.45$ fm, and $V = 40$ MeV, when W was changed from 4 to 3 MeV, there was practically no change in the elastic cross section at $E_{lab} = 49$ MeV and $\theta_{lab} = 170°$, whereas the transfer cross section to $^{89}Y_{g.s.}$ at the same energy and angle increased by almost two orders of magnitude. However, as the value of W approached 10 MeV, this extra sensitivity of the transfer cross section to small changes in W vanished. These results of ours are similar to the observations of Buttle *et al.*[26] in their study of the $^{48}Ca(^{18}O, ^{17}O)^{49}Ca$ reaction with incident energies near the Coulomb barrier.

A comparison of the results for the two well-resolved states in ^{89}Y is particularly disturbing. For the same set of optical parameters, the fit for the 0.91-MeV state seems to be better than that for the ground state of ^{89}Y. In the latter case, theory predicts larger cross sections at higher energies than the experimental results. Excluding the limitations resulting from the nonuniqueness of the optical-potential parameters, which is characteristic of all heavy-ion scattering, a possible reason for this behavior is as follows. Assuming the no-recoil approximation, the allowed angular momentum transfers are $l = 0$ for the ground state of ^{89}Y ($\frac{1}{2}^-$) and $l = 5$ for the first excited state at 0.91 MeV ($\frac{9}{2}^+$). If recoil effects are fully taken into account, the parity selection rule $(-)^{l_1+l_2} = (-)^l$ is no longer valid and the allowed transfers are $l = 0,1$ for the ground state and $l = 4,5$ for the 0.91-MeV state. Since the highest angular momentum transfer allowed typically has the highest yield, this means that if the complete six-dimensional DWBA integral is evaluated, the corresponding relative increase in cross section is expected to be higher for the ground state than for the 0.91-MeV state. While the over-all cross section at all energies is expected to increase with calculations which fully take into account recoil effects, this increase should be smaller at sub-Coulomb energies where the large core-core separations make contributions to the cross sections along the line joining the cores dominant over the off-axis contributions. The longitudinal recoil corrections are approximately taken into account below the barrier by the recipe of Buttle and Goldfarb and the transverse recoil corrections should be negligible by the above argument. The same argument cannot be made about situations above the barrier.

The excitation functions for the unresolved states in ^{141}Pr (Fig. 3) do not show any significant dip characteristic of nuclear distortion even at the highest energies. Sub-Coulomb calculations normalized at $E_{lab} = 59$ MeV seem to reproduce the general trend adequately as seen in Fig. 3. For the unresolved levels at 1.51 and 1.74 MeV in ^{89}Y, the data show effects of nuclear distortion (Fig. 7). With optical-potential sets 1 and 6, fits at higher energies, no worse than those for the $^{89}Y_{g.s.}$ case, are obtained for these unresolved levels assuming spectroscopic factors with the same relative strengths as those quoted by Picard and Bassani.[9] In addition, it is worth mentioning that theoretical cross sections for transfer to the 1.74-MeV level is almost an order of magnitude smaller than that for transfer to the 1.51-MeV level even with the assumption of a maximum spectroscopic factor of unity for the latter. However, in spite of our inability to resolve these levels cleanly at any energy, as is evident from inspection of Fig. 5, the approximate relative yield for the 1.74-MeV level seems more than that predicted from theory.

The main lesson we draw from these comparisons between calculations and experiment above the Coulomb barrier is that in this region the uncertainties of the analysis multiply. Undoubtedly, one could improve the fits we have obtained by allowing greater flexibility of potentials and parameters; but it is clear that we have crossed the threshold into the realm of optical modeling with all its attendant mystique.

VIII. CONCLUSIONS

We conclude by examining how well this study has answered the questions posed in the Introduction.

Concerning our first question, to what extent is the sub-Coulomb DWBA theory an accurate tool and over what range of energies does it appear valid, we can say that there is a range of low bombarding energies where the experimental excitation functions are well matched by the sub-Coulomb DWBA calculations and that over this same range the deviation is negligible between the sub-Coulomb calculations and those that incorporate nuclear distortion. We believe our largest source of theoretical uncertainty lies in the Buttle-Goldfarb approximate treatment of recoil. Comparison of the Coulomb-corrected excitation functions calculated in the post and prior representation suggests that this uncertainty is of the order of only 20%; this matter will not be settled, however, until calculations are available in which recoil is treated without approximation.

In order to discuss what spectroscopic information may be derived from these analyses, we first must note that the invariant quantity fixed by normalizing experiment to calculation, namely, the joint probability $P(R_1, R_2)$, is a function of the spectroscopic factors and bound-state geometric parameters of both the donor and acceptor nuclei.

Only when assumptions are made concering values of these parameters and $S^{(1)}$, the spectroscopic factor of the donor, may we extract values for $S^{(2)}$, the spectroscopic factor of the acceptor. Reasonable assumptions for these parameters and $S^{(1)}$ do lead to values for $S^{(2)}$ which are close to expectation and to those extracted from reactions induced by light ions. It would be desirable, though, to have available firm, independent information concerning $S^{(1)}$ and the parameters of the donor so that spectroscopic information about the acceptor will be less uncertain.

At bombarding energies such that nuclear distortion plays a role, the agreement between calculation and experiment or between different calculations with optical parameters which yield nearly equivalent elastic excitation functions is less satisfactory. It is likely that a proper treatment of recoil will here bring experiment and calculation into closer accord, particularly for the proton transfer to the ground state of ^{89}Y, but the differences between calculations which use differing sets of optical parameters will remain. The lesson we draw from this is that the most reliable spectroscopic information will be that obtained at bombarding energies below the Coulomb barrier.

As a final point we do note that there are practical limitations which restrict the utility of sub-Coulomb heavy-ion-transfer reactions. The poor energy resolution and typically low cross sections limit the number of nuclei and the number of levels in the same nucleus which can be studied. Further, kinematic considerations lead to inhibited transfer cross sections except for a rather narrow band of Q values (often not physically accessible). These considerations lead us to predict that study of single nucleon transfer induced by heavy ions below the Coulomb barrier will be used primarily as a means for calibrating in select cases the spectroscopic information obtained from transfer reactions induced by light ions.

Note added in proof:

(1) Angular distributions for the reactions ^{88}Sr-(^{16}O, ^{15}N)^{89}Y to the ground and first excited states have been reported by Anantaraman, Katori, and Körner[27] for several bombarding energies in the range 44 through 59 MeV.

(2) A computational mistake has been found which concerns our bound-state parameters. It was our intent that the radius parameters of bound-state potentials be related to the potential radius in a conventional fashion by $R = r_0(A-1)^{1/3}$; in fact, the radii had been computed as $R = r_0 \times (A-2)^{1/3}$. Thus, our calculations actually correspond to decreased values of r_0 when one uses the conventional relation; for example, our "standard" parameters for proton transfer to ^{88}Sr become $r_{01} = 1.173$ and 1.235 fm instead of 1.20 and 1.24 fm, respectively. Alternatively stated, this means that cross sections computed with the conventional relation and the radius parameters as printed will be about 8% larger than those computed with the mistaken convention and, accordingly, the spectroscopic factors with "standard" parameters of Table II, Fig. 3, and Fig. 7 should be reduced by about 8%. We should emphasize, though, that such an alteration causes no significant change in the values of $P(R_1, R_2)$, the invariant of the analyses.

(3) Comparisons have now been made between our calculations, which use the Buttle-Goldfarb approximation for recoil, and finite-range calculations which treat recoil exactly[19] for the case of proton transfer to the ground state of ^{89}Y. (We thank Dr. R. M. DeVries for carrying out the exact finite-range calculations.) With the bound-state parameters $r_{01} = r_{02} = 1.20$ fm, and the standard convention for the relation between radius and radius parameter $a_1 = 0.6$ fm, $a_2 = 0.65$ fm, $V_{so} = 0.0$ MeV, optical-model set 1, but no Coulomb terms in the form factor, the ratios of the exact finite-range to Buttle-Goldfarb cross sections at 170° for the four energies 42.5, 44, 46, and 48 MeV are found to be 1.02, 0.94, 1.02, and 1.03, respectively. These suggest that our calculations with the Buttle-Goldfarb procedure are adequately accurate for energies below the Coulomb barrier. Also it is found that the exact finite-range calculations render inoperative our argument in the sixth paragraph of Sec. VII concerning the possible importance at backward angles of $l = 1$ angular momentum transfers for energies above the barrier.

ACKNOWLEDGMENTS

We would like to thank Dr. M. Hasinoff, D. Potter, and Dr. T. Lewellen for their assistance in data collection during the course of these experiments.

---

*Work supported in part by U. S. Atomic Energy Commission.

†Present address: Laboratoire Rene Bernas, Orsay, France.

‡Present address: Argonne National Laboratory, Argonne, Illinois 60439.

§Present address: Center for Nuclear Studies, University of Texas, Austin, Texas 78712.

¶Permanent address: Bhabha Atomic Research Centre, Trombay, Bombay, India.

[1]G. Breit, M. H. Hull, and R. L. Gluckstern, Phys. Rev. 87, 74 (1952); G. Breit and M. E. Ebel, *ibid.* 103, 679 (1956); G. Breit, K. W. Chun, and H. G. Wahsweiler, Phys. Rev. 133, B404 (1964).
[2]J. C. Hiebert, J. A. McIntyre, and J. G. Couch, Phys. Rev. 138, B346 (1965); R. M. Gaedke, K. S. Toth, and I. R. Williams, Phys. Rev. 141, 996 (1966).
[3]J. G. Couch, J. A. McIntyre, and J. C. Hiebert, Phys. Rev. 152, 883 (1966).
[4]A. R. Barnett, W. R. Phillips, P. J. A. Buttle, and L. J. B. Goldfarb, Nucl. Phys. A176, 321 (1971). Also see Ref. 26.
[5]B. H. Wildenthal, E. Newman, and R. L. Auble, Phys. Rev. C 3, 1199 (1971).
[6]W. P. Jones, L. W. Borgman, K. T. Hecht, John Bardwick, and W. C. Parkinson, Phys. Rev. C 4, 580 (1971).
[7]C. D. Kavaloski, J. S. Lilley, D. C. Shreve, and N. Stein, Phys. Rev. 161, 1107 (1967).
[8]B. M. Preedom, E. Newman, and J. C. Hiebert, Phys. Rev. 166, 1156 (1968).
[9]J. Picard and G. Bassani, Nucl. Phys. A131, 636 (1969).
[10]M. M. Stautberg, J. J. Kraushaar, and B. W. Ridley, Phys. Rev. 157, 977 (1967).
[11]P. J. A. Buttle and L. J. B. Goldfarb, Nucl. Phys. 78, 409 (1966); A115, 461 (1968).
[12]T. Sawaguri and W. Tobocman, J. Math, Phys. 8, 2223 (1967); F. Schmittroth, W. Tobocman, and A. A. Golestaneh, Phys. Rev. C 1, 377 (1970).
[13]D. Trautmann and K. Alder, Helv. Phys. Acta 43, 363 (1970); K. Alder and D. Trautmann, Ann. Phys. (N.Y.) 66, 884 (1971).
[14]R. A. Broglia and A. Winther, Nucl. Phys. A182, 112 (1972).
[15]P. J. A. Buttle and L. J. B. Goldfarb, Nucl. Phys. A176, 299 (1971).
[16]Fortran-IV computer code DWUCK and instructions written by P. D. Kunz, University of Colorado (unpublished).
[17]RDRC code. Same as Ref. 12.
[18]F. D. Becchetti, P. R. Christensen, V. I. Manko, and R. J. Nickles, Phys. Lett. 43B, 279 (1973).
[19]R. M. DeVries and K. I. Kubo, Phys. Rev. Lett. 30, 325 (1973).
[20]M. A. Nagarajan, Nucl. Phys. A196, 34 (1972).
[21]J. S. Blair, Phys. Rev. 108, 827 (1957).
[22]J. Rapaport and K. Kerman, Nucl. Phys. A119, 641 (1968).
[23]J. C. Hiebert, E. Newman, and R. H. Bassel, Phys. Rev. 154, 898 (1967).
[24]T. T. S. Kuo and G. E. Brown, Nucl. Phys. 85, 40 (1966).
[25]C. A. Wiedner, A. Heusler, J. Solf, and J. P. Wurm, Nucl. Phys. A103, 433 (1967).
[26]P. J. A. Buttle, J. L. Durell, L. J. B. Goldfarb, J. S. Lilley, and W. R. Phillips, J. Phys. (Paris) 33, 54 (1972).
[27]N. Anantaraman, K. Katori, and H. J. Körner, ANL Physics Division Informal Report No. PHY-1973 B (unpublished), p. 403; and to be published.